Report on recrystallisation of barite in presence of radium

SLOW PROCESSES IN CLOSE-TO-EQUILIBRIUM CONDITIONS FOR RADIONUCLIDES IN WATER/SOLID SYSTEMS OF RELEVANCE TO NUCLEAR WASTE MANAGEMENT

SKIN

DELIVERABLE D2.2

COLLABORATIVE PROJECT (CP)

Grant agreement N°.: FP7-269688

Submitting organizations: FZJ
Authors: Martina Klinkenberg, Felix Brandt, Uwe Breuer, Dirk Bosbach
Due date of deliverable: Project Month 34
Actual submission: Project Month 36

Start date of the project: 01 January 2011
Duration: 36 months

Project co-funded by the European Commission under the Seventh Framework Programme of the European Atomic Energy Community (Euratom) for nuclear research and training activities (2007 to 2011)		
Dissemination Level		
PU	Public	×
RE	Restricted to a group specified by the partners of the project	
CO	Confidential, only for partners of the project	

RECRYSTALLIZATION OF BARITE IN THE PRESENCE OF RADIUM

Martina Klinkenberg[1*], Felix Brandt[1], Uwe Breuer[2], Dirk Bosbach[1]

[1] Forschungszentrum Jülich, Institute of Energy and Climate Research (IEK-6) Nuclear Waste Management and Reactor Safety, (GER)

[2] Forschungszentrum Jülich, Central Institute for Engineering, Electronics and Analytics (ZEA-3) Analytics, (GER)

...

* Corresponding author: m.klinkenberg@fz-juelich.de

A microanalytical approach was applied in order to distinguish between two possible scenarios for the uptake of Ra by already existent barite, (1) formation of a $Ba_{1-x}Ra_xSO_4$ solid solution surface layer on the barite or (2) a complete recrystallization, leading to homogenous $Ba_{1-x}Ra_xSO_4$ crystals. It could be clearly shown that all barite particles analyzed within this study contain Ra not only on their surfaces but within the grains. In addition, the role of Ra during the recrystallization of barite was examined via detailed SEM investigations.

In conclusion, the addition of Ra to a barite at close to equilibrium conditions has a major impact on the system leading to a fast re-equilibration to a $Ba_{1-x}Ra_xSO_4$ solid solution and visible effects on the particle size distribution, even at room temperature.

1. Introduction

The possible solubility control of Ra by coprecipitation of a $Ba_{1-x}Ra_xSO_4$ solid solution has been demonstrated in several cases e.g. Doerner & Hoskins, 1925. However, an open question is whether a Ra containing solution will equilibrate with solid $BaSO_4$

under repository relevant conditions due to barite recrystallization. Here, Ra enters a system in which barite is in equilibrium with the aqueous solution. Previous studies have revealed that uptake of Ra is not limited by pure adsorption at close to equilibrium conditions but involves a significant fraction of the bulk solid (Bosbach et al. 2010, Curti et al. 2010).

Here we present new experimental results, following a combined microscopic and microanalytical approach. Batch experiments were carried out in order to analyze the spatial distribution of Ra within the solid after the recrystallization experiments as well as the effect of the presence of Ra on the morphology and particle size distribution (PSD).

2. Materials and methods

2.1 Sample preparation and characterization

For the Ra uptake experiments, a synthetic, high purity barite (XR-HR10) from Sachtleben Chemie® GmbH was used, which was provided by Enzo Curti (Paul Scherrer Institute PSI, Villingen, Switzerland). The same barite was used in the experiments of [2] and [3]. XRD confirmed that the powder is pure barite within the precision of this method.

A coarse fraction of the Sachtleben barite was separated. The specific surface area of the separated fraction as determined via Kr-BET was S_{BET} = 0.17 m²/g. The separated sample consisted of blocky crystals with a particle size of > 10 µm. The morphology was dominated by barite cleavage planes.

2.2 Experimental setup

Batch recrystallization experiments were performed at ambient conditons (23 ± 2 °C). The barites were pre-treated for 4 weeks in 10 mL of 0.2 n NaCl solutions in 25 mL glass bottles. Afterwards, 10 mL of a Ra^{2+} containing solution were added, resulting in a total volume of 20 mL, an ionic strength of 0.1 n NaCl, and a concentration of $5.0 \cdot 10^{-6}$ mol/L $^{226}Ra^{2+}$. The ionic strength was chosen to be comparable to granitic ground waters e.g. at the Äspö site in Sweden. Experiments were carried out with a solid/liquid

ratio of 5 g/L and 0.5 g/L. In regular time intervals 500 µL of the aqueous solution were taken and then filtered. The liquid was filtered through Advantec ultrafilters (MWCO = 10,000 Da) and then analyzed for the Ra and Ba concentration.

2.3 Analysis of aqueous solutions and solids

The Ra concentration in solution was examined via Gamma spectrometry using a N_2 cooled high purity (HP) Ge-detector. The Ba concentration in solution was quantified via ICP-MS using an ICP-MS ELAN 6100 DRC (PerkinElmer SCISX) instrument.

The morphology of the barite crystals was studied using the environmental scanning electron microscope FEI Quanta 200 F. In order to avoid artifacts due to precipitation of NaCl, $BaSO_4$ or $RaSO_4$, the samples were separated from their solution by two washing steps in iso-propanol. The samples were then prepared as a suspension on a Si wafer and subsequently dried.

From the SEM images, the PSD was determined. For the AL samples, the longest axis of 360 grains of each sample was measured via image analysis of SEM images at 40,000 x and 20,000 x magnifications. Due to the lager grain size of the SL barite and narrow grain size distribution, 150 grains per SL sample were analyzed. Grains, which were grown together, were regarded as single grain. The equivalent mass of each grain was calculated using the measured grain size as the diameter of an equivalent sphere and the density of barite (4.5 g/cm³).

Within this study, a powder method was developed specifically for the analysis of the recrystallized barite and the detection of Ra in the sub-ppm range by time of flight secondary ion mass spectroscopy (TOF-SIMS). The spatial distribution of Ra and Ba within the recrystallized barite powders was analyzed using an ION-TOF instrument. For the mass spectral analysis a pulsed Bi^{3+} beam of 25 keV was used. The raw data were reconstructed and analyzed using the ION-TOF software package.

3. Results and discussion

3.1 Final Ra concentration in aqueous solution

The Ra concentration in solution significantly decreased during 443 days of experiment. The final concentrations are given in Table 2. The experiments with 5 g/L barite the Ra concentration showed a decrease from 5.0 x 10^{-6} to the order of 10^{-9} mol/L whereas the Ra concentration in solution of the 0.5 g/L experiments decreased to the order of 10^{-08} mol/L. According to these results, a Ra/Ba ratio of the solid was calculated from mass balance. A Ra/Ba = 2.5 x 10^{-4} was calculated for the experiments with S/L = 5 g/L barite whereas for S/L = 0.5 g/L barite the Ra/Ba ratio was calculated to be one order of magnitude higher (Figure 1).

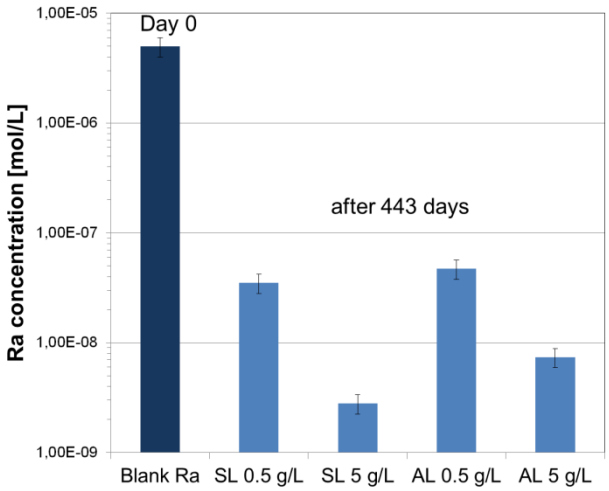

Figure 1: *Final Ra concentrations after 443 days.*

3.2 TOF-SIMS investigations

Due to the grain size, the SL sample was chosen for a detailed ToF-SIMS investigation of the spatial distribution of Ra and the total Ra/Ba ratio. After these adjustments, individual grains could be identified by comparing a SEM image taken before the measurement (Figure 4 a) with the integrated intensity distribution image of Ba (Figure 4 b) and Ra (Figure 4 c). In addition, measurements were carried out with the AL-type barite with a focus on the Ra/Ba ratio of the grains.

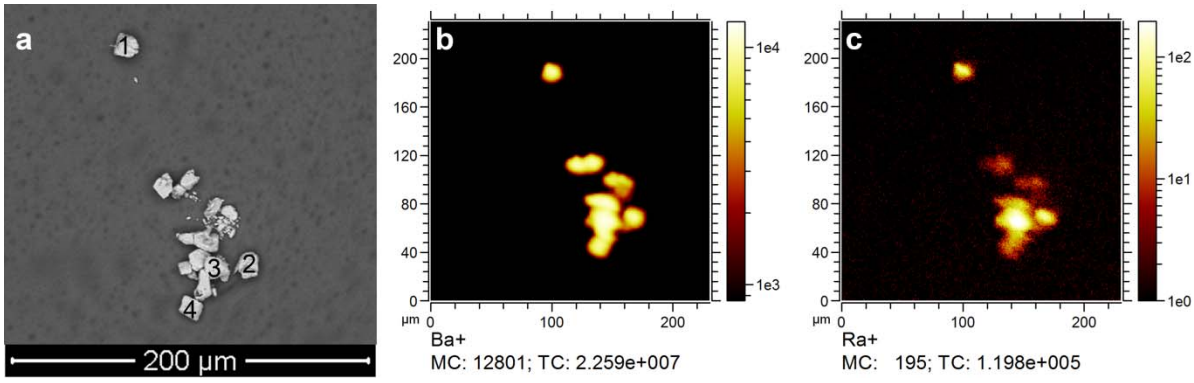

Figure 2: *a) SEM image of SL 0.5 g/L before the TOF-SIMS analysis. Depth profiles of numbered grains (1 -4) are shown in Figure 5, b) integrated intensity of the Ba signal c) integrated intensity of the Ra signal. MC = Maximum Counts, TC = Total counts.*

A comparison of the images showing the integrated Ba and Ra ToF-SIMS signal (Figure 2 b) and the SEM images shows a good correlation between the areas of high integrated intensities in the ToF-SIMS images and the spatial distribution of the grains in the SEM image. Furthermore, it can be seen in Figure 2 that all grains within this measurement of the recrystallized SL barite contain Ra.

Four grains were identified in the ToF-SIMS image and depth profiles were created using the IONTOF software (Figure 3). The profiles indicate a complete recrystallization of barite to a $Ba_{1-x}Ra_xSO_4$ solid solution on the scale of the ToF-SIMS instrument. All SL grains which were analyzed indicate measurable concentrations of Ra not only on the surface but also within the grains. The total Ra concentration within the grains varies as can be seen by the total counts depicted in Figure 5.

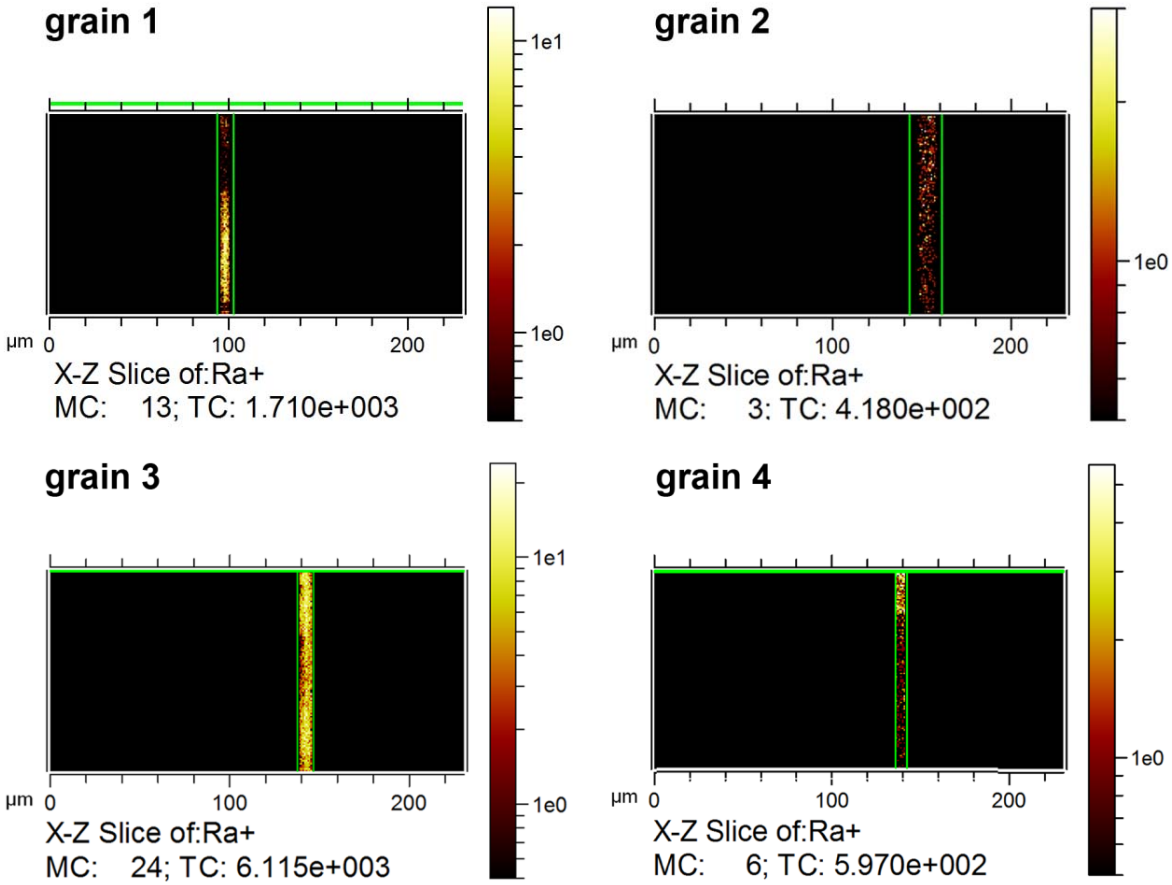

Figure 3: *Depth profiles of the integrated Ra signal (MC = Maximum Counts, TC = Total counts) obtained from the grains depicted in Figure 2.*

The Ba/Ra ratio was calculated from several TOF-SIMS measurements, using the integrated elemental signals (Fig. 3 c). Mass balance calculations for the Sachtleben barite suggest a mole fraction of $X_{RaSO4}(s) = 2.3 \times 10^{-3}$, assuming full recrystallization at the end of the ex-periment. The Ra/Ba intensity distribution of Fig. 4 has its maximum between 2 and 4×10^{-3}, corresponding well with the macroscopic results.

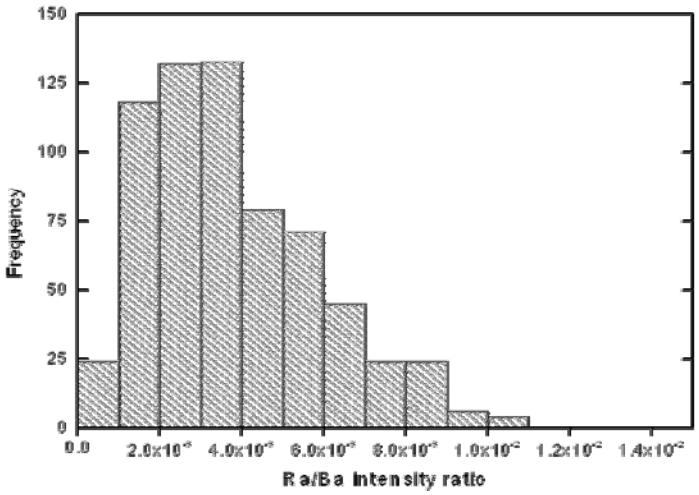

Figure 4: *Evaluation of Ra/Ba intensities as calculated from the TOF-SIMS measurements. The calculated Ra/Ba based on mass balance is 2.3 . 10^{-3}.*

3.3 Evolution of the particle size distribution due to recrystallization in the presence of Ra

Particle size distributions (PSD) were determined to quantify the observations by SEM with more extended statistical information about the ensemble of barite particles. The initial AL type barite is characterized by a wide PSD, covering more than one order of magnitude in the mass based representation (Figure 10, Table 3). A slight shift of the PSD towards higher grain sizes was observed on the AL reference sample which was aged for 443 days which is more clearly detected in the frequency based PSD. Mainly, the very small grains in the fraction < 500 nm were shifted to the fraction 500 – 1000 nm (Figure 10, left). In the presence of Ra, not only new large grains appeared as described above but also a significant coarsening of the small grains can be deduced from the PSD shown in Figure 10. The most significant effect is visible in the mass based PSD of the 0.5 g/L AL sample where the fraction < 500 nm has almost completely vanished (Figure 10, right).

The original SL barite sample is characterized by a narrow grain size distribution with grain sizes between ~ 6 and 45 µm (Table 1; Figure 11, left). No measurable changes in the PSD could be detected without Ra due to aging. Even in the presence of Ra, the

narrow grain size distribution remains mainly unchanged with insignificant differences between minimum and maximum values of the PSD (Figure 11, right; Table 3). Therefore, it can be concluded that a wide PSD is the precondition for a significant PSD coarsening effect. However, the connected grains as shown in Figure 8 were considered individually for the PSD. The main coarsening mechanism for the SL barite is the formation of aggregates which might eventually grow together to from large grains. Such effects were also observed by Jia & Goa, 2008 (23), who investigated the growth of well-defined cubic hematite single crystals due to the oriented aggregation of particles and Ostwald ripening. Here, particles formed agglomerates which eventually made up single crystals.

Table 1: *Overview of grain sizes at the beginning and end of the experiments of SL and AL barite.*

	Minimum	Maximum	Mean value	
			Frequency based	Equ. mass based
	[µm]	[µm]	[µm]	[µm]
AL Reference at the beginning	0.19	2.20	0.50	0.69
AL Reference 5 g/L after 443 days	0.19	2.97	0.58	0.82
AL 5 g/L after 443 days	0.28	3.58	0.80	1.15
AL 0.5 g/L after 443 days	0.25	3.59	0.86	1.26
		360 grains per sample analyzed		
	[µm]	[µm]	[µm]	[µm]
SL Reference at the beginning	5.62	44.65	15.00	18.62
SL 5 g/L after 443 days	5.46	38.13	15.28	18.79
SL 0.5 g/L after 443 days	5.91	44.64	14.99	18.33
		150 grains per sample analyzed		

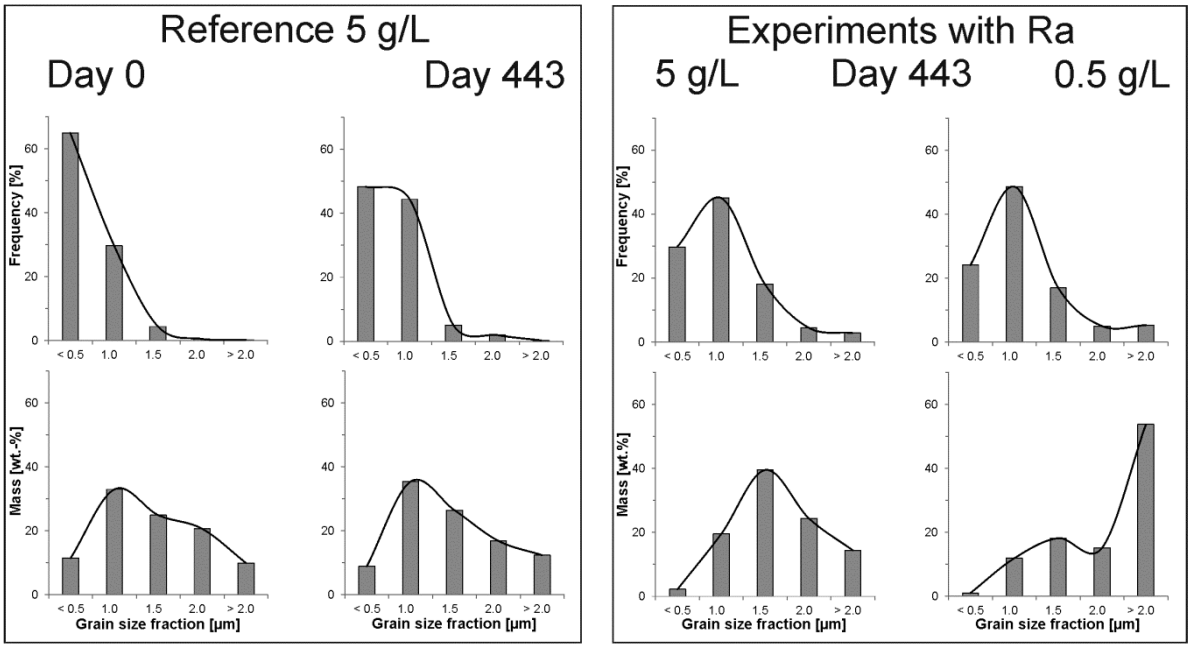

Figure 5: *PSD based on frequency (upper histograms) and equivalent mass (lower histograms) of AL barite. Left: Experiments without Ra (Reference); right: Experiments with Ra.*

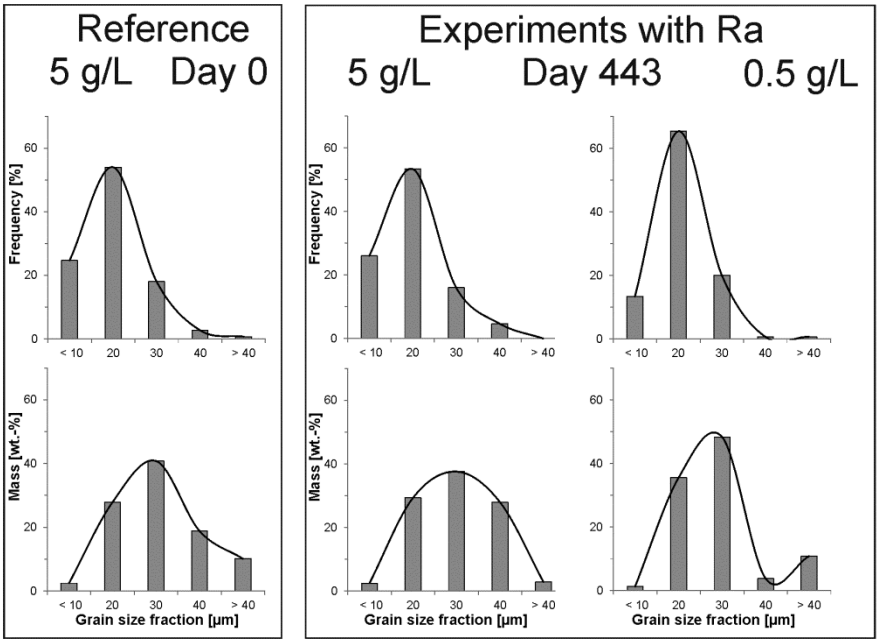

Figure 11. Comparison of the PSD of SL reference sample without Ra at the beginning of the experiment with the end point of the Ra uptake experiments with 5 g/L and 0.5 g/L barite after 443 days.

Conclusions

ToF-SIMS results clearly show that all barite particles analyzed within this study contain Ra not only on their surfaces but within the grains. For most grains, a homogenous distribution of Ra could be determined. Therefore, a complete recrystallization of barite into a $Ba_{1-x}Ra_xSO_4$ solid solution can be proposed. From the intensities of Ra and Ba obtained during the ToF-SIMS, Ra/Ba intensity ratio distributions were computed. The maxima of the histograms are identical with the expected Ra/Ba ratio calculated from mass balance under the assumption of complete recrystallization.

In summary, two different effects of the presence of Ra can be observed, depending on the original PSD. The wide PSD of AL barite is significantly altered during the recrystallization of barite in the presence of Ra compared to a Ra free reference. On the other hand, the particle size of the SL sample with a narrow PSD remains more or less

constant. Here, eventually a coarsening due to the presence of Ra is expected due to the formation of new grains from intergrown agglomerates.